UNIVERSITY *of* York

This is a repository copy of *Search for C violation in the decay η → π0e+e− with WASA-at-COSY*.

White Rose Research Online URL for this paper:
https://eprints.whiterose.ac.uk/135818/

Version: Published Version

White Rose
university consortium
Universities of Leeds, Sheffield & York

eprints@whiterose.ac.uk
https://eprints.whiterose.ac.uk/

Search for C violation in the decay $\eta \to \pi^0 e^+ e^-$ with WASA-at-COSY

The WASA-at-COSY Collaboration

P. Adlarson [a], W. Augustyniak [b], W. Bardan [c], M. Bashkanov [d], F.S. Bergmann [e,*],
M. Berłowski [f], A. Bondar [g,h], M. Büscher [i,j], H. Calén [a], I. Ciepał [k], H. Clement [l,m],
E. Czerwiński [c], K. Demmich [e], R. Engels [n], A. Erven [o], W. Erven [o], W. Eyrich [p], P. Fedorets [n,q],
K. Föhl [r], K. Fransson [a], F. Goldenbaum [n], A. Goswami [n,s], K. Grigoryev [n,t], C.-O. Gullström [a],
L. Heijkenskjöld [a,1], V. Hejny [n], N. Hüsken [e], L. Jarczyk [c], T. Johansson [a], B. Kamys [c],
G. Kemmerling [o,2], G. Khatri [c,3], A. Khoukaz [e], A. Khreptak [c], D.A. Kirillov [u], S. Kistryn [c],
H. Kleines [o,2], B. Kłos [v], W. Krzemień [f], P. Kulessa [k], A. Kupść [a,f], A. Kuzmin [g,h], K. Lalwani [w],
D. Lersch [n], B. Lorentz [n], A. Magiera [c], R. Maier [n,x], P. Marciniewski [a], B. Mariański [b],
H.-P. Morsch [b], P. Moskal [c], H. Ohm [n], W. Parol [k], E. Perez del Rio [l,m,4], N.M. Piskunov [u],
D. Prasuhn [n], D. Pszczel [a,f], K. Pysz [k], A. Pyszniak [a,c], J. Ritman [n,x,y], A. Roy [s], Z. Rudy [c],
O. Rundel [c], S. Sawant [z], S. Schadmand [n], I. Schätti-Ozerianska [c], T. Sefzick [n], V. Serdyuk [n],
B. Shwartz [g,h], K. Sitterberg [e], T. Skorodko [l,m,aa], M. Skurzok [c], J. Smyrski [c], V. Sopov [q],
R. Stassen [n], J. Stepaniak [f], E. Stephan [v], G. Sterzenbach [n], H. Stockhorst [n], H. Ströher [n,x],
A. Szczurek [k], A. Trzciński [b], M. Wolke [a], A. Wrońska [c], P. Wüstner [o], A. Yamamoto [ab],
J. Zabierowski [ac], M.J. Zieliński [c], J. Złomańczuk [a], P. Żuprański [b], M. Żurek [n]

and

A. Wirzba [n,ad]

[a] Division of Nuclear Physics, Department of Physics and Astronomy, Uppsala University, Box 516, 75120 Uppsala, Sweden
[b] Department of Nuclear Physics, National Centre for Nuclear Research, ul. Hoza 69, 00-681, Warsaw, Poland
[c] Institute of Physics, Jagiellonian University, Prof. Stanisława Łojasiewicza 11, 30-348 Kraków, Poland
[d] School of Physics and Astronomy, University of Edinburgh, James Clerk Maxwell Building, Peter Guthrie Tait Road, Edinburgh EH9 3FD,
United Kingdom of Great Britain and Northern Ireland
[e] Institut für Kernphysik, Westfälische Wilhelms-Universität Münster, Wilhelm-Klemm-Str. 9, 48149 Münster, Germany
[f] High Energy Physics Department, National Centre for Nuclear Research, ul. Hoza 69, 00-681, Warsaw, Poland
[g] Budker Institute of Nuclear Physics of SB RAS, 11 Akademika Lavrentieva prospect, Novosibirsk, 630090, Russia
[h] Novosibirsk State University, 2 Pirogova Str., Novosibirsk, 630090, Russia
[i] Peter Grünberg Institut, PGI-6 Elektronische Eigenschaften, Forschungszentrum Jülich, 52425 Jülich, Germany
[j] Institut für Laser- und Plasmaphysik, Heinrich-Heine Universität Düsseldorf, Universitätsstr. 1, 40225 Düsseldorf, Germany
[k] The Henryk Niewodniczański Institute of Nuclear Physics, Polish Academy of Sciences, Radzikowskiego 152, 31-342 Kraków, Poland
[l] Physikalisches Institut, Eberhard-Karls-Universität Tübingen, Auf der Morgenstelle 14, 72076 Tübingen, Germany
[m] Kepler Center für Astro- und Teilchenphysik, Physikalisches Institut der Universität Tübingen, Auf der Morgenstelle 14, 72076 Tübingen, Germany
[n] Institut für Kernphysik, Forschungszentrum Jülich, 52425 Jülich, Germany
[o] Zentralinstitut für Engineering, Elektronik und Analytik, Forschungszentrum Jülich, 52425 Jülich, Germany
[p] Physikalisches Institut, Friedrich-Alexander-Universität Erlangen-Nürnberg, Erwin-Rommel-Str. 1, 91058 Erlangen, Germany
[q] Institute for Theoretical and Experimental Physics named by A.I. Alikhanov of National Research Centre "Kurchatov Institute", 25 Bolshaya Cheremushkinskaya,
Moscow, 117218, Russia
[r] II. Physikalisches Institut, Justus-Liebig-Universität Gießen, Heinrich-Buff-Ring 16, 35392 Giessen, Germany

* Corresponding author.
  E-mail address: florianbergmann@uni-muenster.de (F.S. Bergmann).
[1] Present address: Institut für Kernphysik, Johannes Gutenberg-Universität Mainz, Johann-Joachim-Becher Weg 45, 55128 Mainz, Germany.
[2] Present address: Jülich Centre for Neutron Science JCNS, Forschungszentrum Jülich, 52425 Jülich, Germany.
[3] Present address: Department of Physics, Harvard University, 17 Oxford St., Cambridge, MA 02138, USA.
[4] Present address: INFN, Laboratori Nazionali di Frascati, Via E. Fermi, 40, 00044 Frascati, Roma, Italy.

[s] *Department of Physics, Indian Institute of Technology Indore, Khandwa Road, Simrol, Indore – 453552, Madhya Pradesh, India*
[t] *High Energy Physics Division, Petersburg Nuclear Physics Institute named by B.P. Konstantinov of National Research Centre "Kurchatov Institute",*
1 mkr. Orlova roshcha, Leningradskaya Oblast, Gatchina, 188300, Russia
[u] *Veksler and Baldin Laboratory of High Energy Physics, Joint Institute for Nuclear Physics, 6 Joliot-Curie, Dubna, 141980, Russia*
[v] *August Chełkowski Institute of Physics, University of Silesia, Uniwersytecka 4, 40-007, Katowice, Poland*
[w] *Department of Physics, Malaviya National Institute of Technology Jaipur, JLN Marg Jaipur – 302017, Rajasthan, India*
[x] *JARA–FAME, Jülich Aachen Research Alliance, Forschungszentrum Jülich, 52425 Jülich, and RWTH Aachen, 52056 Aachen, Germany*
[y] *Institut für Experimentalphysik I, Ruhr-Universität Bochum, Universitätssstr. 150, 44780 Bochum, Germany*
[z] *Department of Physics, Indian Institute of Technology Bombay, Powai, Mumbai – 400076, Maharashtra, India*
[aa] *Department of Physics, Tomsk State University, 36 Lenina Avenue, Tomsk, 634050, Russia*
[ab] *High Energy Accelerator Research Organisation KEK, Tsukuba, Ibaraki 305-0801, Japan*
[ac] *Astrophysics Division, National Centre for Nuclear Research, Box 447, 90-950 Łódź, Poland*
[ad] *Institute for Advanced Simulation and Jülich Center for Hadron Physics, Forschungszentrum Jülich, 52425, Germany*

A R T I C L E   I N F O

A B S T R A C T

We report on the search for the rare decay $\eta \rightarrow \pi^0 e^+ e^-$ which is of interest to study C violation in the electromagnetic interaction which would indicate contributions from physics beyond the Standard Model, since the allowed decay via a two-photon intermediate state is strongly suppressed. The experiment has been performed using the WASA-at-COSY installation, located at the COSY accelerator of the Forschungszentrum Jülich, Germany. In total 3×10^7 events of the reaction pd $\rightarrow {}^3$Heη have been recorded at an excess energy of $Q = 59.8$ MeV. Based on this data set the C parity violating decay $\eta \rightarrow \pi^0 \gamma^* \rightarrow \pi^0 e^+ e^-$ via a single-photon intermediate state has been searched for, resulting in new upper limits of $\Gamma\left(\eta \rightarrow \pi^0 e^+ e^-\right) / \Gamma\left(\eta \rightarrow \pi^+ \pi^- \pi^0\right) < 3.28 \times 10^{-5}$ and $\Gamma\left(\eta \rightarrow \pi^0 e^+ e^-\right) / \Gamma\left(\eta \rightarrow \text{all}\right) < 7.5 \times 10^{-6}$ (CL = 90%), respectively.

1. Introduction

According to the standard model, strong and electromagnetic interactions have to conserve C parity. This concept particularly restricts the decay modes of mesons and, as an instance, highly suppresses $\eta \rightarrow \pi^0 e^+ e^-$. However, corresponding measurements of the relative branching ratio date back to the seventies of the last century and their sensitivity is limited to many orders of magnitudes above the standard model predictions. The process $\eta \rightarrow \pi^0 e^+ e^-$ via the single-photon intermediate state $\eta \rightarrow \pi^0 \gamma^*$ would violate C parity conservation whereas a two-photon process as a physical background has an expected branching ratio not larger than 10^{-8} according to theoretical calculations [1–3].

A modern model for this process includes the coupling of a hypothetical massive dark U boson [4–6] to the virtual photon where the corresponding interaction strength scales with $\sim \epsilon^2 q^2 / (q^2 - m_U^2 + i m_U \Gamma_U)$ rather than with $\sim q^2 / (q^2 + i \varepsilon) \sim 1$ as in case of a photon propagator. Here, q^2 denotes the momentum transfer square of the photon, m_U and Γ_U are the U boson mass and total width, respectively, and ϵ is the coupling constant of the γ–U interaction. A search for a resonance peak structure resulting from the considered η decay is limited to a U boson mass $m_U \leq m_\eta - m_{\pi^0} = 413$ MeV/c^2. However, in this letter results based on a vector meson dominance model (VMD) for a decay via a virtual photon will be presented. In case of the decay $\eta \rightarrow \pi^0 \gamma^* \rightarrow \pi^0 e^+ e^-$ the VMD model is dominated by the ρ meson with a mass of $m_\rho = 775.26(25)$ MeV/c^2 [7]. Further details about the used VMD model are given in Refs. [8,9].

Apparently, the η meson is well suited for the study of rare processes and the search for C, P and CP breaking decays, since it is not only a C and P eigenstate of strong and electromagnetic interaction but all strong and electromagnetic decays of the η meson are either suppressed or forbidden to first order. Nevertheless, the present experimental upper limit for the branching ratio of the decay $\eta \rightarrow \pi^0 e^+ e^-$ was obtained in 1975 with an optical spark chamber experiment and amounts only to 4.5×10^{-5} (CL = 90%) [10]. To determine a more stringent upper limit for the decay channel $\eta \rightarrow \pi^0 e^+ e^-$, data collected with the WASA-at-COSY facility have been analyzed which also constituted the basis for studies of other η meson decay channels already published in Ref. [11].

2. Experiment

The WASA-at-COSY experiment was an internal experiment operated at the accelerator COSY of the Forschungszentrum Jülich, Germany from 2006 to 2014 [12]. For the measurements discussed here, a proton beam was accelerated to a kinetic beam energy of $T_p = 1$ GeV and collided with deuterium pellets provided by the internal pellet target. The η mesons were produced in the reaction pd $\rightarrow {}^3$Heη.

The WASA detector setup is divided into two main parts. The central detector, which was used for the reconstruction of the produced mesons and their decay particles, consists of a drift chamber in a solenoid field surrounded by an electromagnetic calorimeter. This setup provided an energy resolution of 3% for charged and 8% for neutral particles as well as a geometrical acceptance of 96%. The forward detector used for the measurement of the four-momenta of the forward scattered ^{3}He nuclei comprised several layers of thin and thick plastic scintillators enabling particle identification and energy reconstruction with a 3% accuracy as well as a proportional chamber giving precise angular information with 0.2% accuracy. A more detailed description of the WASA-at-COSY experimental setup can be found in Refs. [11–13].

The data for the studies presented here were obtained in two measurement periods, one of four weeks in 2008 and one of eight weeks in 2009. A large energy loss in subsequent scintillator elements of the forward detector was required to trigger the data acquisition. Since the ^{3}He nucleus stemming from the reaction pd $\rightarrow {}^3$Heη is stopped in the first layer of the WASA forward range hodoscope, a veto on the signals from the second layer was used

in addition. Due to the trigger relying on information from the forward detector only, the utilized trigger was unbiased with respect to a decay mode of the η meson. In total about 3×10^7 events containing an η meson were recorded with 1×10^7 events originating from the 2008 period and 2×10^7 events from the 2009 period [11].

3. Data analysis

The analysis of the decay $\eta \to \pi^0 e^+ e^-$ was based on a common analysis chain for η decay studies described in Ref. [11].

Preselection. Before the selection conditions for the decay $\eta \to \pi^0 e^+ e^-$ were determined, the data collected in 2008 and 2009 were preselected with conditions common to all recorded reactions. For instance, conditions on time correlations were used, requiring charged and neutral particles to be detected within a time window of less than 40 ns and 15 ns, respectively, compared to the ^{3}He nucleus measured in the forward detector. Furthermore, hits that were wrongly identified as additional particles (so-called split-offs) are rejected. Electron–positron pairs from photon conversion at the COSY beam pipe can be identified by a reconstructed vertex more than 28 mm off the COSY beam axis and by a reconstructed invariant mass below 8 to 15 MeV/c^2, depending on the reconstructed radial vertex position and assuming a vertex at the COSY beam pipe. Those pairs are rejected, as well. More details of these conditions were published in Ref. [11].

Besides these general preselection conditions, a cut on the signature of the decay $\eta \to \pi^0 e^+ e^-$ was applied requesting at least one positively and one negatively charged particle detected in the central detector, as well as at least two neutral particles originating from the π^0 meson decay $\pi^0 \to \gamma\gamma$. The last condition applied for data preselection requires the maximum considered momenta of the charged decay particles to be below $p = 250$ MeV/c, since the momenta of the leptons of the decay $\eta \to \pi^0 e^+ e^-$ are expected to be below this value.

Monte Carlo simulations. In order to determine optimal selection conditions for the search for the decay channel $\eta \to \pi^0 e^+ e^-$, 1.8×10^8 Monte Carlo events of all non-signal η decays observed yet were created with respect to their relative branching ratio [7], as well as two million events for the signal decay. These simulations were generated with the PLUTO++ software package [14] considering the angular distribution of pd $\to$ ^{3}Heη at $T_p = 1$ GeV according to Ref. [15]. For the various η decay channels physics models as included in PLUTO++ were used. The reader is referred to Ref. [11] for further details.

In addition to the simulations of η decays, about 4.3×10^9 events for the direct pion production were created, with most events for the production reactions pd $\to$ ^{3}He$\pi^0\pi^0$ and pd $\to$ ^{3}He$\pi^+\pi^-$, as these contribute most to the non-η background at the given kinetic beam energy. For these two-pion productions the ABC effect was incorporated into the simulations according to the model discussed in Ref. [16].

The simulations for the signal decay $\eta \to \pi^0 e^+ e^-$ were generated with two different model assumptions. The first one is a decay according to pure three-particle phase space. The second is based on the VMD model for the intermediate virtual photon. The direct decay $\eta \to \pi^0 \gamma$ to an *on-shell* photon violates both C parity and angular momentum conservation plus global gauge invariance. The violation of the angular momentum originates from the general rule that a radiative $0 \to 0$ transition via the emission or absorption of a real photon is strictly forbidden, as can be read in more detail in Ref. [17]. The global gauge invariance is the reason that the divergence of the electromagnetic $\eta\pi^0$ transition
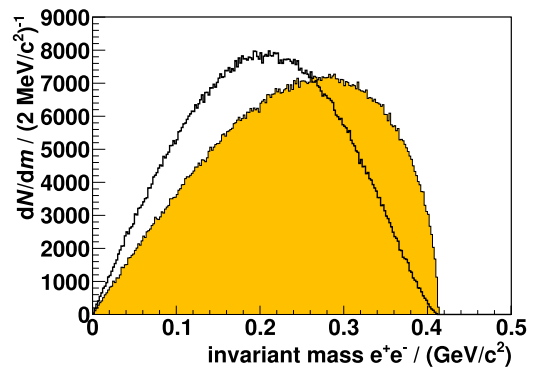

Fig. 1. Invariant mass of e^+e^- pairs for the simulated decay $\eta \to \pi^0 e^+ e^-$. Black lined: decay via $\eta \to \pi^0 \gamma^*$ considering VMD. Shadowed in orange: decay according to three-particle phase space. (For interpretation of the colors in the figure(s), the reader is referred to the web version of this article.)

current has to vanish. This in turn implies that the on-shell limit of the $\eta\pi^0$ coupling to a photon has to vanish as well, since the only term that is not directly proportional to q^2 corresponds to a longitudinally polarized photon, which therefore cannot contribute to an on-shell-photon amplitude, see e.g. [18] for more details. In summary, there is no $\eta \to \pi^0 \gamma$ on-shell contribution for the decay $\eta \to \pi^0 e^+ e^-$ and the transition form factor for the off-shell contribution vanishes at zero virtuality, such that the single-photon pole is completely removed [19–21]. In Fig. 1 the invariant mass of the e^+e^- pair produced in the decay is plotted according to three-particle phase space (shadowed in orange) and the decay via $\eta \to \pi^0 \gamma^*$ according to the discussed model. A more detailed calculation of the model can be found in Ref. [9].

To simulate the WASA detector responses, the WASA Monte Carlo package WMC was used, which is based on GEANT3 [22]. The settings for the spatial, timing and energy resolution in WMC were set to agree with the resolution observed in data.

Due to the high luminosities of the WASA-at-COSY experiment, it is possible that detector responses from one event can overlap with another event. In Ref. [11] the event selection was done without taking this effect into account. Any remaining effect on the relative branching ratios reported was checked by studying the luminosity dependence of the result. However, for the analysis presented in this paper event overlap could not be ignored, because it influences all differential distributions which were used for event selection and cut optimization. Therefore, the effect was considered in the simulations and the amount of event overlap was left as a free parameter for the fit of the simulations to data (see next paragraph).

All Monte Carlo simulations were preselected with conditions identical to those for data preselection.

Data description. The choice of the selection conditions with regard to the decay channel $\eta \to \pi^0 e^+ e^-$ is based on Monte Carlo simulations. It is necessary to know the contributions of the various reactions to the collected data for an optimal choice. Therefore, the 2008 and 2009 data sets were fitted separately in distributions of selected quantities by template distributions of the aforementioned Monte Carlo simulations to determine the contributions of the individual reactions to the data. In detail, these distributions are:

- the missing mass m_X, corresponding to the invariant mass of the proton beam and the deuteron target remaining after the ^{3}He four momentum has been subtracted and peaks at the η mass for the reaction pd $\to$ ^{3}Heη,

- the invariant mass $m_{ee\gamma\gamma}$ of an electron–positron pair candidate and two photons, which peaks at the η mass for the decay $\eta \to \pi^0 e^+ e^-$ with $\pi^0 \to \gamma\gamma$,
- the invariant mass $m_{\gamma\gamma}$ of two photons, which peaks at the π^0 mass for reactions with π^0 mesons produced,
- the invariant mass m_{ee} of an electron–positron pair candidate,
- the smallest invariant mass $m_{e\gamma}$ of all four possible combinations of an electron or positron candidate and a photon and
- the missing mass squared m^2_{Xee}, which is the invariant mass squared of the proton beam and the deuteron target remaining after the ^{3}He four momentum and the electron–positron pair candidate momentum have been subtracted and peaks at the π^0 mass squared for the reaction of interest.

Under the assumption of a branching ratio of the decay below the current upper limit of 4.5×10^{-5} (CL = 90%) [10], there are less than 150 events expected from the decay $\eta \to \pi^0 e^+ e^-$ in the combined data sets after preselection, considering the preselection efficiency for the signal decay. A fit by Monte Carlo simulations including the simulated decay $\eta \to \pi^0 e^+ e^-$ is consistent with zero events from this signal decay channel. Therefore, the decay $\eta \to \pi^0 e^+ e^-$ was excluded from the fit. While the differential distribution for the reaction pd $\to$ ^{3}Heη is well known [15], the differential distributions are known only with high uncertainties or not at all for direct multi-pion productions. Hence, the data were divided into ten bins in angular ranges of $\cos\vartheta^{cms}_{^3He}$.[5] Monte Carlo simulations were fitted to data in the eight angular bins ranging from -1 to 0.6. The angular range $0.6 < \cos\vartheta^{cms}_{^3He} \le 1$ was excluded because of the lower energy resolution of the forward detector for these forward scattered ^{3}He nuclei. Moreover, the relative amount of background from the direct pion production is larger in this angular range, whereas less than 3% of all pd $\to$ ^{3}Heη events have a $\cos\vartheta^{cms}_{^3He} > 0.6$.

The fit of the Monte Carlo simulations to the data was performed simultaneously for all angular ranges and distributions with identical scaling parameters for the simulations for all distributions within one angular range. Furthermore, the ratios for the various η decays were constrained to the branching ratios according to Ref. [7] within the given uncertainties. These were set to be identical for all angular ranges. Similarly, the amount of event overlap was included as one global fit parameter. In Fig. 2, Fig. 3, Fig. 4 and Fig. 5 the resulting Monte Carlo fits to the 2008 data are plotted for m_X, $m_{ee\gamma\gamma}$, $m_{\gamma\gamma}$ and m_{ee} for the angular range $0.2 < \cos\vartheta^{cms}_{^3He} \le 0.4$. According to this fit most events remaining after preselection originate from the η decay $\eta \to \pi^+\pi^-\pi^0$, the direct pd $\to$ ^{3}He$\pi^+\pi^-\pi^0$ production and the direct two-pion production reactions. Note that MC simulations with event overlap are required for a proper description of the shoulders of the invariant mass distributions. A collection of all fits is available in Ref. [9].

Selection conditions. The selection conditions for the search for the decay $\eta \to \pi^0 e^+ e^-$ were based on the following quantities:

- the missing mass m_X,
- the invariant masses $m_{ee\gamma\gamma}$, $m_{\gamma\gamma}$ and m_{ee},
- the χ^2 probability of a kinematic fit with the hypothesis pd $\to$ ^{3}He$\gamma\gamma e^+ e^-$ and
- the energy loss E^{SEC}_{dep} of the charged particles in the central detector scintillator electromagnetic calorimeter (SEC) and their momentum p to discriminate $e^\pm$ and $\pi^\pm$ (particle identification, PID).

---

[5] $\vartheta^{cms}_{^3He}$ is the polar scattering angle of the ^{3}He nucleus relative to the beam axis in the center of mass system.

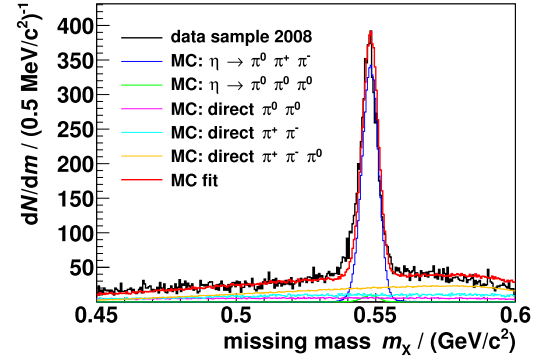**Fig. 2.** Missing mass $m_X = |\mathbb{P}_p + \mathbb{P}_d - \mathbb{P}_{^3He}|$ after preselection for a data sample of the 2008 period fitted by Monte Carlo simulations. Only the most common contributions of the various reactions to the fit are plotted separately.
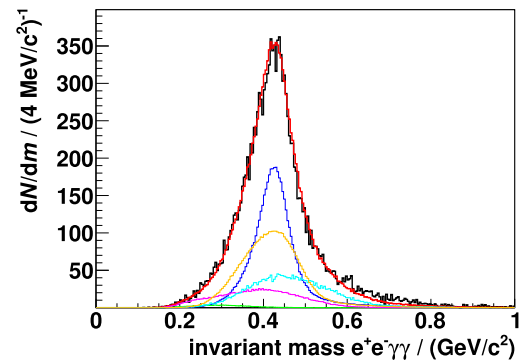

Fig. 3. Invariant mass of $e^+ e^- \gamma\gamma$ after preselection for a data sample of the 2008 period fitted by Monte Carlo simulations. For the legend see Fig. 2.
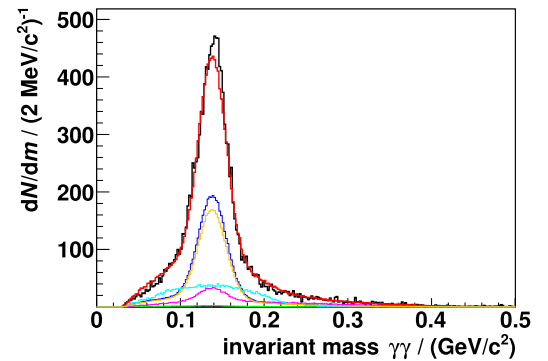

Fig. 4. Invariant mass of $\gamma\gamma$ after preselection for a data sample of the 2008 period fitted by Monte Carlo simulations. For the legend see Fig. 2.

Since only very few events were expected to remain in the analysis after the event selection, an optimal choice of the selection conditions is important for the best possible result. The choice of the cut conditions was performed with 40% of the generated Monte Carlo simulations, whereas the remaining Monte Carlo data sample was used later for the selection efficiency determination. Note that the relative amounts of the different reaction channels are the same for both MC samples, scaled according to the fit explained in the previous paragraph. The graphical cut for the particle identification (see Fig. 6) was chosen by optimizing the product of the number of selected $e^+ e^-$ pairs ($N_{e^+e^-}$) and the ratio of $N_{e^+e^-}$ to the number of charged pion pairs ($N_{\pi^+\pi^-}$). While this cut was chosen beforehand, as it is a common cut utilized for PID independent from the analyzed reaction, the selection conditions
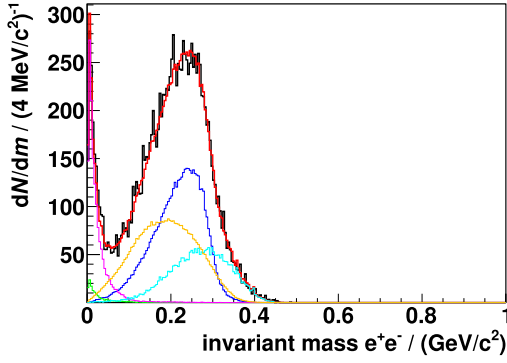
Fig. 5. Invariant mass of e^+e^- after preselection for a data sample of the 2008 period fitted by Monte Carlo simulations. For the legend see Fig. 2.
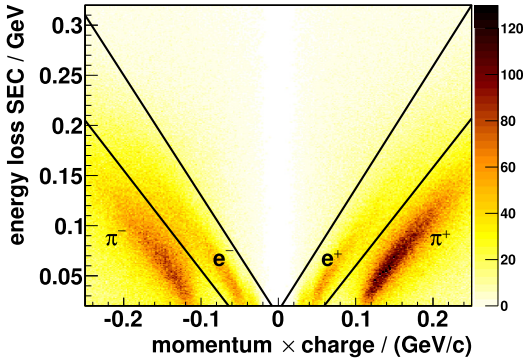

Fig. 6. Energy loss of charged particles in the SEC plotted against their momentum times charge for the preselected data sets of the 2008 and 2009 periods. A graphical cut around the electron and positron band is indicated by black lines.

for the other five quantities were determined by an optimization algorithm. This algorithm is based on the relative amount of simulated signal events $S_R = N_S^{cut}/N_S^{pres}$ remaining after all cuts (N_S^{cut}) compared to the number after preselection (N_S^{pres}) and the relative amount of all simulated background events $B_R = N_B^{cut}/N_B^{pres}$ remaining after all cuts (N_B^{cut}) in relation to the number after preselection (N_B^{pres}). In case of the background reactions the contributions as obtained in the data description were used to downscale the Monte Carlo simulations and to extract the numbers.

The cut optimization algorithm maximizes the evaluation function

$$G = S_R \cdot \frac{S_R}{B_R} \tag{1}$$

by varying the selection conditions for all chosen quantities. This way an optimal signal to background ratio is achieved while at the same time an optimal number of remaining signal events can be obtained.

With the aid of the cut optimization algorithm the following selection conditions were determined:

$$0.5414 \,\text{GeV}/c^2 \leq \quad m_X \quad \leq 0.5561 \,\text{GeV}/c^2, \tag{2}$$

$$0.507 \,\text{GeV}/c^2 \leq \quad m_{ee\gamma\gamma} \quad \leq 0.646 \,\text{GeV}/c^2, \tag{3}$$

$$0.0923 \,\text{GeV}/c^2 \leq \quad m_{\gamma\gamma} \quad \leq 0.1574 \,\text{GeV}/c^2, \tag{4}$$

$$m_{ee} \quad \geq 0.096 \,\text{GeV}/c^2 \text{ and} \tag{5}$$

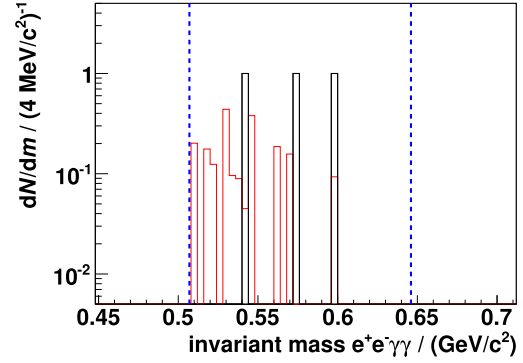$$\chi^2 \text{ prob.} \quad \geq 0.05. \tag{6}$$

Fig. 7. Invariant mass of $e^+e^-\gamma\gamma$ after all cuts for the 2008 and 2009 data sets (black) and for the simulations scaled to data according to the fit to data after preselection (red). The blue dashed lines indicate the chosen selection conditions.

4. Results

After applying the selection conditions to the data, three events were left, whereas two events were expected to remain from the direct two-pion production $pd \rightarrow {}^3\text{He}\pi^0\pi^0$ according to Monte Carlo simulations. All other background reaction channels were found to give no sizeable contribution after applying the cuts. The invariant mass, $m_{ee\gamma\gamma}$, for these events are plotted in Fig. 7 together with simulated data. Note that the generated Monte Carlo events were scaled according to the fit to data after preselection and that the sum of all Monte Carlo events remaining after all cuts is equal to two events.

The overall reconstruction efficiency for the signal decay $\eta \rightarrow \pi^0 e^+e^-$ was determined to be

$$\varepsilon_S^{\text{virtual}} = 0.02331(7) \tag{7}$$

for a decay via $\eta \rightarrow \pi^0\gamma^*$ assuming VMD, whereas the assumption of a decay according to pure three-particle phase space results in

$$\varepsilon_S^{\text{phase}} = 0.01844(7). \tag{8}$$

The given uncertainties are purely statistical ones.

In order to calculate the upper limit for the branching ratio $\Gamma(\eta \rightarrow \pi^0 e^+e^-)/\Gamma(\eta \rightarrow \text{all})$, the decay channel $\eta \rightarrow \pi^+\pi^-\pi^0$ with $\pi^0 \rightarrow \gamma\gamma$ was utilized for normalization. This is a reasonable choice as this decay channel has the same signature as the signal decay and, thus, possible systematic effects introduced by differences of the signature are avoided. According to the data description by Monte Carlo simulations and considering the efficiency correction factors for the preselection of

$$\varepsilon_{\eta \rightarrow \pi^+\pi^-\pi^0_{\gamma\gamma}, 2008}^{\text{pres.}} = 0.03587(26) \tag{9}$$

determined by Monte Carlo studies for the data set collected in 2008 and

$$\varepsilon_{\eta \rightarrow \pi^+\pi^-\pi^0_{\gamma\gamma}, 2009}^{\text{pres.}} = 0.03305(18) \tag{10}$$

for the data set collected in 2009 there were

$$N_{\eta \rightarrow \pi^+\pi^-\pi^0_{\gamma\gamma}}^{\text{produced}} = (6.509 \pm 0.018) \times 10^6 \tag{11}$$

events in data. In order to determine a final upper limit for the branching ratio of $\eta \rightarrow \pi^0 e^+e^-$, all uncertainties have to be considered and incorporated into the calculations.

Systematics. The systematic and statistical uncertainties, which need to be considered for the upper limit determination, can be
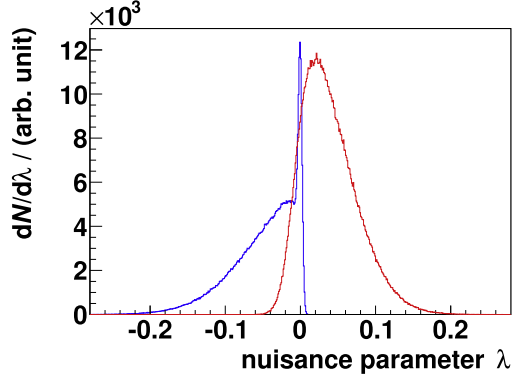
Fig. 8. Nuisance parameters λ_{2008} (red) and λ_{2009} (blue) for the systematic uncertainty of the number of background events remaining after all cuts in the 2008 and 2009 data sets.

separated into uncertainties by multiplicative effects and uncertainties by offset effects. The former include an uncertainty of the reconstruction efficiency of the decay $\eta \to \pi^0 e^+ e^-$ and an uncertainty in the number of $\eta \to \pi^+\pi^-\left(\pi^0 \to \gamma\gamma\right)$ events in data. The latter ones are uncertainties of the number of background events remaining after all cuts.

To determine the systematic uncertainty for the signal reconstruction efficiency, the resolution settings for the Monte Carlo simulations were varied within the uncertainties of the individual detector resolutions observed in data. The extracted square root of the relative variance of the reconstruction efficiency was found to be

$$\sqrt{\mathrm{Var}_{\mathrm{rel}}^{\mathrm{virtual}}} = 0.059 \tag{12}$$

for a decay via $\eta \to \pi^0\gamma^*$ assuming VMD whereas for a decay according to pure three-particle phase space one finds

$$\sqrt{\mathrm{Var}_{\mathrm{rel}}^{\mathrm{phase}}} = 0.057. \tag{13}$$

In the following analysis the square root of the variance was considered as the systematic uncertainty.

The uncertainty for the efficiency corrected number of $\eta \to \pi^+\pi^-\left(\pi^0 \to \gamma\gamma\right)$ events in data was obtained by a comparison to the efficiency corrected number determined utilizing less strict preselection conditions, namely no cuts to reject conversion or split-off events, no cut on the momentum of charged decay particles and less strict cuts on the particles' energies. Hereby a systematic uncertainty of 2.3% was determined.

The uncertainties for the number of background events remaining after all cuts can be separated into a statistical uncertainty due to the finite number of Monte Carlo simulations and systematic uncertainties introduced by uncertainties of the fit of Monte Carlo simulations to data. The latter are dominated by differences between the Monte Carlo fit parameters for the 2008 and 2009 data sets, leading to asymmetric uncertainties. Such different fit parameters for both data sets originated mainly from different experimental settings, which affected, e.g., the event overlap due to different luminosities. To determine the overall systematic uncertainty for the number of remaining background events, the probability density functions (pdf) of the individual uncertainties were folded. The resulting pdf for the nuisance parameters λ_{2008} and λ_{2009} corresponds to the overall relative systematic uncertainty for the 2008 and 2009 data sets and was incorporated into the upper limit calculations. In Fig. 8 the distribution of the nuisance parameters are illustrated for both data sets.

In order to investigate further possible systematic effects, the selection conditions used for the analysis were varied and the

expectations according to simulations were compared to the number of events seen in data. Since the expected number of events agreed with the number of events seen in data within the statistical uncertainties, no additional systematic effect needs to be considered.

A detailed description of the uncertainty investigations is available in Ref. [9].

Upper limit. The upper limit for the relative branching ratio of the decay $\eta \to \pi^0 e^+ e^-$ was calculated with the formula:

$$\frac{\Gamma\left(\eta \to \pi^0 e^+ e^-\right)}{\Gamma\left(\eta \to \pi^+\pi^-\pi^0\right)} < \frac{N_{\mathrm{S,up}}}{N_{\eta\to\pi^+\pi^-\pi^0}^{\mathrm{produced}} \cdot \varepsilon_{\mathrm{S}}} \tag{14}$$

with the upper limit $N_{\mathrm{S,up}}$ for the number of signal events, which depends on the number of observed events and the number of expected background events. For the calculation of $N_{\mathrm{S,up}}$ a Bayesian approach was chosen as given in Ref. [23] with a flat prior pdf and incorporating the determined uncertainties and the pdfs for the nuisance parameters, resulting in

$$N_{\mathrm{S,up}} = 4.97 \qquad (\mathrm{CL} = 90\%). \tag{15}$$

As a result the relative branching ratio of the decay $\eta \to \pi^0 e^+ e^-$ via $\eta \to \pi^0\gamma^*$ and assuming VMD was found to be

$$\frac{\Gamma\left(\eta \to \pi^0 e^+ e^-\right)_{\mathrm{virtual}}}{\Gamma\left(\eta \to \pi^+\pi^-\pi^0\right)} < 3.28 \times 10^{-5} \qquad (\mathrm{CL} = 90\%) \tag{16}$$

whereas the assumption of a pure three-particle phase space distribution of the ejectiles results in

$$\frac{\Gamma\left(\eta \to \pi^0 e^+ e^-\right)_{\mathrm{phase}}}{\Gamma\left(\eta \to \pi^+\pi^-\pi^0\right)} < 4.14 \times 10^{-5} \qquad (\mathrm{CL} = 90\%). \tag{17}$$

Considering the branching ratio of the decay $\eta \to \pi^+\pi^-\pi^0$ of $\Gamma\left(\eta \to \pi^+\pi^-\pi^0\right)/\Gamma\left(\eta \to \mathrm{all}\right) = 0.2292(28)$ [7], the new upper limit for the branching ratio of the decay $\eta \to \pi^0 e^+ e^-$ via $\eta \to \pi^0\gamma^*$ results in

$$\frac{\Gamma\left(\eta \to \pi^0 e^+ e^-\right)_{\mathrm{virtual}}}{\Gamma\left(\eta \to \mathrm{all}\right)} < 7.5 \times 10^{-6} \qquad (\mathrm{CL} = 90\%). \tag{18}$$

For comparison the assumption of a pure three-particle phase space distribution of the ejectiles would lead to

$$\frac{\Gamma\left(\eta \to \pi^0 e^+ e^-\right)_{\mathrm{phase}}}{\Gamma\left(\eta \to \mathrm{all}\right)} < 9.5 \times 10^{-6} \qquad (\mathrm{CL} = 90\%). \tag{19}$$

These values are smaller than the previous upper limit of 4.5×10^{-5} ($\mathrm{CL} = 90\%$) [10] by a factor of six and five, respectively.

5. Summary

We have presented new studies with the WASA-at-COSY experiment on the C parity violating η meson decay $\eta \to \pi^0 e^+ e^-$. The obtained upper limit for the branching ratio of the decay $\eta \to \pi^0 e^+ e^-$ is smaller than the previously available upper limit by a factor of five to six [10]. The results of the analysis are consistent with no events seen in data, and thus give no hint on a C violation in an electromagnetic process. Similarly, no processes from physics beyond the Standard Model are required to explain the results.

In order to further decrease this value and to continue the search for a C parity violation in an electromagnetic process, additional data were collected with WASA-at-COSY utilizing the pro-

duction reaction pp → ppη. Over three periods in 2008, 2010 and 2012 in total about 5×10^8 such events were recorded and are currently being analyzed with regard to the decay $\eta \to \pi^0 e^+ e^-$.

Besides a decay via one virtual photon according to a VMD model, the decay $\eta \to \pi^0 e^+ e^-$ could possibly occur via a hypothetical C violating dark boson U where the pertinent form factor is even further suppressed by $\epsilon^2 q^2 / (q^2 - m_U^2 + i m_U \Gamma_U)$ compared to the single-photon mechanism without a U [24]. Investigations with regard to this decay process are currently ongoing for the presented pd → ^{3}Heη data sets and the pp → ppη data sets recorded with WASA-at-COSY providing an order of magnitude higher statistics.

Acknowledgements

References

[1] T.P. Cheng, Phys. Rev. 162 (1967) 1734–1738, https://doi.org/10.1103/PhysRev.162.1734.

[2] J. Smith, Phys. Rev. 166 (1968) 1629–1632, https://doi.org/10.1103/PhysRev.166.1629.

[3] J.N. Ng, D.J. Peters, Phys. Rev. D 47 (1993) 4939–4948, https://doi.org/10.1103/PhysRevD.47.4939.

[4] P. Fayet, Phys. Lett. B 95 (1980) 285–289, https://doi.org/10.1016/0370-2693(80)90488-8.

[5] M.I. Dobroliubov, A.Y. Ignatiev, Phys. Lett. B 206 (1988) 346–348, https://doi.org/10.1016/0370-2693(88)91519-5.

[6] L.B. Okun', Sov. Phys. JETP 56 (1982) 502–505.

[7] C. Patrignani, et al., Chin. Phys. C 40 (2016) 100001, https://doi.org/10.1088/1674-1137/40/10/100001.

[8] T. Petri, Master's thesis, Rheinische Friedrich-Wilhelms-Universität Bonn, Germany, 2010, arXiv:1010.2378.

[9] F.S. Bergmann, Ph.D. thesis, Westfälische Wilhelms-Universität Münster, Germany, 2017.

[10] M.R. Jane, et al., Phys. Lett. B 59 (1975) 99–102, https://doi.org/10.1016/0370-2693(75)90167-7.

[11] P. Adlarson, et al., Phys. Rev. C 94 (2016) 065206, https://doi.org/10.1103/PhysRevC.94.065206.

[12] B. Hoistad, J. Ritman, et al., WASA-at-COSY Collaboration, arXiv:nucl-ex/0411038, 2004.

[13] C. Bargholtz, et al., Nucl. Instrum. Methods A 594 (2008) 339–350, https://doi.org/10.1016/j.nima.2008.06.011.

[14] I. Fröhlich, et al., PoS ACAT2007 (2007) 076, arXiv:0708.2382.

[15] P. Adlarson, et al., Eur. Phys. J. A 50 (2014) 100, https://doi.org/10.1140/epja/i2014-14100-4.

[16] P. Adlarson, et al., Phys. Rev. C 91 (2015) 015201, https://doi.org/10.1103/PhysRevC.91.015201.

[17] J.J. Sakurai, Invariance Principles and Elementary Particles, Princeton University Press, Princeton, New Jersey, 1964.

[18] E. Leader, E. Predazzi, J. Phys. G 40 (2013) 075001, https://doi.org/10.1088/0954-3899/40/7/075001.

[19] J. Bernstein, G. Feinberg, T.D. Lee, Phys. Rev. 139 (1965) B1650–B1659, https://doi.org/10.1103/PhysRev.139.B1650.

[20] B. Barrett, et al., Phys. Rev. 141 (1966) 1342–1349, https://doi.org/10.1103/PhysRev.141.1342.

[21] M.J. Bazin, et al., Phys. Rev. Lett. 20 (1968) 895–898, https://doi.org/10.1103/PhysRevLett.20.895.

[22] R. Brun, et al., CERN Report No. W5013, 1994, URL http://cds.cern.ch/record/1082634.

[23] Y. Zhu, Nucl. Instrum. Methods A 578 (2007) 322–328, https://doi.org/10.1016/j.nima.2007.05.116.

[24] A. Kupść, A. Wirzba, J. Phys. Conf. Ser. 335 (2011) 012017, https://doi.org/10.1088/1742-6596/335/1/012017.